·Clinical Research·

Multifocal electroretinogram in non-pathological myopic subjects: correlation with optical coherence tomography

Ai-Ping Song, Tao Yu, Jian-Rong Wang, Wei Liu, Yan Sun, Su-Xiang Ma

Department of Ophthalmology, Second People's Hospital, Jinan 250001, Shandong Province, China

Correspondence to: Wei Liu. Department of Ophthalmology, Second People's Hospital, Jinan 250001, Shandong Province, China. sapwl@hotmail.com

Received: 2014-09-26 Accepted: 2015-05-13

Abstract

• AIM: To investigate the changes of retinal function in non-pathological myopic subjects using multifocal electroretinography (mfERG) and to correlate the data with the central macular thickness obtained using optical coherence tomography (OCT).

• METHODS: One hundred and thirteen subjects (113 eyes) with age range from 18 to 35y were enrolled in the study. The subjects were divided into four groups according to spherical equivalent (SE) and axial length (AL): emmetropia group (EG, *n*=31; SE: +0.75 to −0.50 D; AL: 22 to 24 mm), low and medium myopia group (LMMG, *n*=26; SE: >−0.50 to −6.00 D; AL: >24 to 26 mm), high myopia group (HMG, *n*=34; SE: >−6.00 to −10.00 D; AL: >26 to 28 mm) and super high myopia group (SHMG, *n*=22; SE: >−10.00 D; AL: >28 mm). The P1 amplitude density, P1 amplitude, and P1 implicit time of the first-order kernel mfERG responses were obtained and grouped into five rings. The central subfield macular thickness (CST) was obtained using macular cube 512×218 scan of Cirrus HD-OCT.

• RESULTS: With the increasing of eccentricity, the first positive peak (P1) amplitude density (*P*=0.0000, 0.0001, 0.0021 in ring 1-3 respectively) and P1 amplitude (all *P*=0.0000 in ring 1-5) of each group decreased. With the increasing of myopia, P1 implicit time gradually extended (all *P*=0.0000 in ring 1-3). The average CST in four diagnostic groups was 241.56±12.72 μm, 244.56±12.19 μm, 254.33±11.61 μm, 261.75±11.83 μm respectively. With the increasing of myopia, CST increased (*P*<0.001). There was negative relationship between CST and P1 amplitude, P1 amplitude density (*r*=−0.402, *P*<0.001; *r*=−0.261, *P*=0.003). There was positive relationship between CST and P1 implicit time (*r*=0.34, *P*<0.001).

• CONCLUSION: With the increasing of myopia, P1 amplitude density and P1 amplitude of the first-order reaction gradually reduced. This showed potential decline in retinal function in myopia. To some extent it may reflect the functional disorder or depression of the visual cells. The exact mechanism needs further study.

• **KEYWORDS:** multifocal electroretinogram; optical coherence tomography; myopia

DOI:10.18240/ijo.2016.02.21

Song AP, Yu T, Wang JR, Liu W, Sun Y, Ma SX. Multifocal electroretinogram in non-pathological myopic subjects: correlation with optical coherence tomography. *Int J Ophthalmol* 2016;9(2):286-291

INTRODUCTION

Myopia is the most common eye disorder. The prevalence of myopia has increased yearly in East Asia [1-2]. Chinese adults had higher prevalence of myopia, high myopia as well as the longer axial length (AL) when compared with non-Chinese adults [3]. Myopia occurs when the AL of the eye is too long for its optical power and the increased AL is the principal anatomical feature that differentiates myopia from emmetropia [4]. Previous studies have shown the retina is thinner in myopes [5] and in the tree shrew with induced myopia [6]. This structual thinning was recently found to link with reduced retinal function in humans[7].

The multifocal electroretinography (mfERG) was introduced by Sutter and Tran (1992) and has been used to investigate a number of eye conditions [8]. The mfERG uses a pseudorandom binary m-sequence to stimulate multiple retinal areas to give a topographic array of retinal responses[9].

Most previous studies reported the mfERG due to pathological changes, and few have investigated the variation in myopia, especially non-pathological myopia. Non-pathological myopia, also known as simple myopia, is caused by excessive near vision. Non-pathological myopia is defined as no myopic retinal changes and can be corrected to normal vision by using appropriate lenses. Here we examined the first-order responses of the mfERG in emmetropes and non-pathological myopes. The aim of this study was to investigate retinal function in non-pathological myopia and to correlate the electrophysical assessment of the retina with the mfERG and the anatomical evaluation of the retina performed by the optical coherence tomography (OCT).

SUBJECTS AND METHODS

Subjects One hundred and thirteen Chinese subjects who met the inclusion criteria were examined during the period from June 2013 to December 2013 in the Department of Ophthalmology, the Second People's Hospital of Jinan, Shandong Province, China. All subjects completed a full ophthalmic examination, including best corrected vision acuity (BCVA), refraction, intraocular pressure (IOP) measured by Goldmann applanation tonometry, gonioscope examination, visual field, dilated fundus examinations, and central macular thickness measurement using optical coherence tomograghy (Cirrus HD-OCT 4000, Soft version 6.0, Carl Zeiss Meditec Inc., Dublin, USA). Subjects without other eye disorders except for refraction errors and BCVA above 20/25 were included in the study. Subjects were divided into four groups according to their spherical equivalent (SE) and AL: emmetropia group (EG, n=31; SE: +0.75 to -0.50 D; AL: 22 to 24 mm), low and medium myopia group (LMMG, n =26; SE: ＞-0.50 to -6.00 D; AL: ＞24 to 26 mm), high myopia group (HMG, n=34; SE: ＞-6.00 to -10.00D; AL: ＞26 to 28 mm) and super high myopia group (SHMG, n=22; SE: ＞-10.00 D; AL: ＞28 mm).

Subjects with the pathological form of myopia, with signs of myopic retinal degenerations (*e.g.* central or peripheral chorioretinal degeneration, posterior staphyloma, neovascularization) were not included in the study. Subjects with clinical evidence of concurrent diseases other than refractive error, such as glaucoma, media opacity, uveitis, retinal diseases or histories of intraocular surgery, refractive surgery, neurologic diseases, and diabetes were excluded. Subjects who met the inclusion criteria with both eyes had one eye randomly selected for mfERG. This study was conducted in accordance with the ethical standards stated in the Declaration of Helsinki and approved by the Ethics Committee of the Second People's Hospital of Jinan, Shandong Province, China, with informed consent obtained from all participants.

Visual Field Testing Standard visual field testing was performed with the static automated white-on-white threshold 24-2 SITA standard strategy (Humphrey Field Analyzer II; Carl Zeiss Meditec, Inc., Dublin, USA). A visual field was defined as reliable when fixation losses and false-positive and false-negative rates were less than 25%. A visual field defect was defined as having three or more significant (P<0.05) non-edge contiguous points with at least one at the P<0.01 level on the same side of the horizontal meridian in the pattern deviation plot and classified as outside normal limits in the Glaucoma Hemifield Test.

Optical Coherence Tomography OCT was performed with the Cirrus HD-OCT system and macular cube 512×218 protocol. This scan protocol generates a cube of data through a 6-mm square grid by acquiring a series of 128 horizontal scan lines comprising 512 A-scans. This is defined as scans with a signal strength ＞6 that exhibits correct delineation of the retina layers as detected automatically by the intrinsic software segmentation algorithm and without image artifacts caused by eye movement and papillary shadowing. All data were performed by the same operator under the same condition.

Multifocal Electroretinography Measurement MfERG stimulation was performed with the Visual Evoked Response Imaging System (Retiscan, Wiesbaden/Brandenburg, Germany). It is equipped with a CRT stimulator. Responses were recorded monocularly using Jet electrode, which was positioned on the inferior cornea along the lid margin and temporally fixed. The pupil of the eye was dilated (≥8 mm) with tropicamide (0.5%, Santen, Japan) . Gold-cup reference and surface electrodes were applied on the temple and forehead, respectively.

The visual stimulus array was driven at a frame rate of 60 Hz and consisted of 61-scaled hexagons displayed on a monitor subtending 38° horizontally and 29.5° vertically. The size of the hexagons was scaled with eccentricity to elicit approximately equal amplitude responses at all locations. Each hexagon was temporally modulated between black and white according to a pseudorandom binary m-sequence (2^{13}-1 steps in length), with a luminance of 100 cd/m^2 in the white hexagons and 3 cd/m^2 in the black hexagons (measured with a BM-7 luminance colorimeter, Topcon, Tokyo, Japan). Normal room lighting was used (surface luminances: -300 cd/m^2).

Subjects were optically corrected for the viewing distance (50 cm) and they were asked to maintain fixation on the red fixation target at the center of the stimulus matrix and refrain from blinking. Segments containing ERG artefacts due to blinks or small eye movements were discarded and re-recorded. Each session of recording took approximately 4min to complete and was divided into 16 equal segments (each of 10s duration). Data from two full mfERG recording sessions were obtained for each subject and averaged. Retinal signals were band-pass filtered (1-300 Hz), sampled every 1.87ms and amplified (100 000 Grass amplifier).

Waveform Analysis For each waveform, the amplitude and implicit time of the first positive peak (P1) of the first-order kernel were determined (Figure 1). P1 amplitude was measured from the trough of the first negative wave to the peak of the positive wave while the implicit time was measured from stimulus onset to the first prominent response peak.

MfERG data were grouped into five concentric rings, with ring 1 representing the foveal response (central 2°) and rings 2-5 corresponding to the successive annuli of stimulation (ring 2: 2°-7.6°, ring 3: 7.6°-14.8°, ring 4: 14.8°-23°, ring 5: 23°-30°) (Figure 2).

Table 1 Characteristics of emmetropic and myopic subject groups $\bar{x} \pm s$

Parameters	EG (n=31)	LMMG (n=26)	HMG (n=34)	SHMG (n=22)	P
Spherical equivalent diopter (D)	0.00±0.04	-2.49±1.38	-8.53±1.95	-13.88±1.76	<0.001[a]
Axial length (mm)	23.60±0.65	24.39±0.75	26.73±0.97	29.98±1.08	<0.001[a]
Gender (M/F)	14/17	16/10	18/16	9/13	0.41[b]
Age (a)	24.48±5.41	26.62±5.38	24.33±5.70	25.82±5.68	0.3471
Intraocular pressure (mm Hg)	13.7±2.4	13.5±2.2	14.1±2.5	14.0±2.2	0.7600

[a]One-factor analysis of variance; [b]Chi-square test.

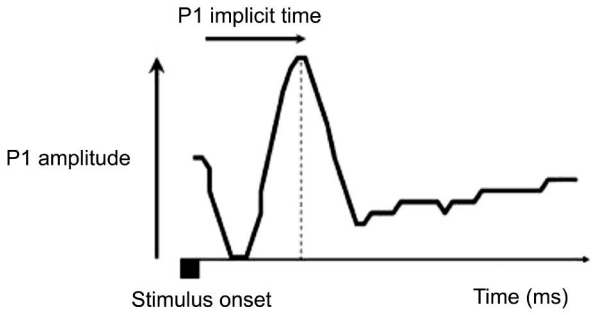

Figure 1 Schematic diagram of a first-order mfERG response Amplitude and implicit time of the waveform are labelled. P1 amplitude is measured from the trough of the first negative wave to the peak of the positive wave. P1 implicit time is measured from stimulus onset to the first prominent response peak.

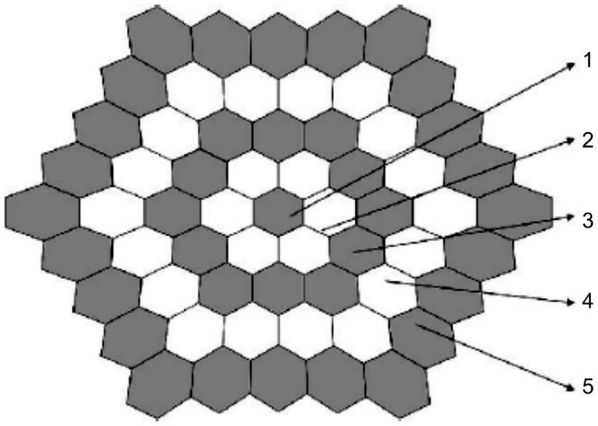

Figure 2 Diagram of the stimulus array used to elicit the mfERG responses Hexagon size increased with retinal eccentricity and responses across the retina were separated into five concentric rings (rings 1-5) for data analysis.

IOL Master Examination We applied light interference biomeasurement equipment (IOL Master, Carl Zeiss Meditec Inc., Dublin, USA) to perform the AL measurement. The patients stared at an inner fixation of the instrument, and we measured AL 3 times and obtained the mean value.

Statistical Analysis Statistical analyses were performed using SPSS 11.5. The differences of P1 amplitude density, P1 amplitude and P1 implicit time among the four diagnostic groups were analyzed by one factor analysis of variance (ANOVA) followed by SNK test (Student-Newman-Keuls test). Pearson's coefficient was used to correlate the parameters obtained from the central ring with the central subfield macular thickness (CST). $P < 0.05$ was considered statistically significant.

RESULTS

High correlation was found between AL and SE (r=0.782, P<0.0005). No significant difference was found in gender distribution among the groups (P=0.41). The average age of EG, LMMG, HMG, and SHMG was 24.48±5.41, 26.62±5.38, 24.33±5.70 and 25.82±5.68y, respectively. The difference of average age among groups was not statistically significant (P=0.3417). The average IOP of EG, LMMG, HMG, and SHMG was 13.7±2.4, 13.5±2.2, 14.1±2.5 and 14.0±2.2 mm Hg respectively. There were no differences between four groups (P=0.76) (Table 1).

With the increasing of eccentricity , P1 amplitude density of each group decreased. The analysis of ANOVA showed the differences of P1 amplitude density among groups were statistically significant in ring 1, ring 2 and ring 3(P=0.0000, 0.0001, 0.0021). SNK test showed that the differences of P1 amplitude density were statistically significant between random two groups in ring 1. The differences of P1 amplitude density were significant between EG and SHMG, LMMG and SHMG, HMG and SHMG in ring 2 (all P< 0.01). The differences of P1 amplitude density were significant between EG and SHMG (P<0.05), LMMG and SHMG (P<0.01) in ring 3. The differences of P1 amplitude density were not statistically significant in ring 4 and ring 5 (P=0.7008, 0.8835) (Table 2).

With the increasing of eccentricity , P1 amplitude in each group decreased. The analysis of ANOVA showed that the differences of P1 amplitude among groups were statistically significant in rings 1-5 (all P=0.0000). Pairwise comparison showed that no significant difference existed between HMG and SHMG (Table 3).

With the increasing of myopia, P1 implicit time gradually extended. Differences of P1 implicit time among groups were statistically significant in ring 1, ring 2 and ring 3 (all P=0.0000). Pairwise comparison showed that the differences between LMMG and HNG were not statistically significant in rings 1-5. The differences were statistically significant between EG and SHMG, LMMG and SHMG, HMG and SHMG in ring 1, ring 2 and ring 3 (Table 4).

With the increasing of myopia, CST increased. The average CST in four diagnostic groups was 241.56±12.72, 244.56± 12.19, 254.33 ±11.61 and 261.75 ±11.83 μm respectively.

Table 2 P1 amplitude density in four groups $\bar{x} \pm s$, nV/deg^2

Parameters	Ring 1	Ring 2	Ring 3	Ring 4	Ring 5
EG (n=31)	130.16±27.89	65.13±11.89	43.09±10.78	26.42±7.42	19.89±6.19
LMMG (n=26)	114.32±25.08	60.87±12.56	40.87±9.56	25.78±8.24	19.08±6.48
HMG (n=34)	95.43±24.18	58.64±15.34	37.54±9.89	24.87±8.76	18.87±6.57
SHMG (n=22)	72.13±22.78	46.84±16.35	32.65±9.56	23.78±9.58	18.54±6.98
P[1]	0.0000	0.0001	0.0021	0.7008	0.8835
Q1	3.3419[a]	1.6106	1.1796	0.4021	0.6597
Q2	7.8466[b]	2.6276	3.1580	1.0427	0.8896
Q3	11.6793[b]	6.5967[b]	5.2919[a]	1.5821	1.0489
Q4	4.0681[b]	0.8606	1.8061	0.5835	0.1746
Q5	8.1714[b]	4.8696[b]	4.0096[b]	1.1534	0.4038
Q6	4.7778[b]	4.3361[b]	2.5253	0.6655	0.2612

[1]One-factor analysis of variance followed by SNK test. Q1: Q values between EG group and LMMG group; Q2: Q values between EG group and HMG group; Q3: Q values between EG group and SHMG group; Q4: Q values between LMMG group and HMG group; Q5: Q values between LMMG group and SHMG group; Q6: Q values between HMG group and SHMG group. [a]P<0.05; [b]P<0.01.

Table 3 P1 amplitude in four diagnostic groups $\bar{x} \pm s$, μV

Parameters	Ring 1	Ring 2	Ring 3	Ring 4	Ring 5
EG (n=31)	1.73±0.44	1.31±0.26	1.16±0.28	1.09±0.2	1.09±0.38
LMMG (n=26)	1.28±0.37	1.09±0.23	1.02±0.2	0.91±0.21	0.98±0.21
HMG (n=34)	0.98±0.42	0.78±0.36	0.76±0.34	0.71±0.28	0.68±0.23
SHMG (n=22)	0.93±0.37	0.72±0.28	0.71±0.31	0.67±0.27	0.63±0.2
P[1]	0.0000	0.0000	0.0000	0.0000	0.0000
Q1	5.9009[b]	4.0110[b]	2.5648	3.9441[b]	2.1565
Q2	10.5318[b]	10.3476[b]	7.8472[b]	8.9164[b]	8.6076[b]
Q3	10.0075[b]	10.2614[b]	7.8643[b]	8.7790[b]	8.6030[b]
Q4	4.0156[b]	5.7692[b]	4.8620[b]	4.4732[b]	6.0035[b]
Q5	4.2133[a]	6.1927[b]	5.2135[b]	4.8276[b]	6.2991[b]
Q6	0.6372	1.0632	0.8903	0.8518	0.9527

[1]One-factor analysis of variance followed by SNK test. Q1: Q values between EG group and LMMG group; Q2: Q values between EG group and HMG group; Q3: Q values between EG group and SHMG group; Q4: Q values between LMMG group and HMG group; Q5: Q values between LMMG group and SHMG group; Q6: Q values between HMG group and SHMG group. [a]P<0.05; [b]P<0.01.

Table 4 P1 implicit time in four diagnostic groups $\bar{x} \pm s$; ms

Parameters	Ring 1	Ring 2	Ring 3	Ring 4	Ring 5
EG (n=31)	39.23±7.53	35.68±5.93	34.93±5.34	37.08±1.98	36.77±2.1
LMMG (n=26)	40.29±6.46	38.5±5.67	36.85±3.1	37.19±3.76	36.8±2.33
HMG (n=34)	42.51±3.91	40.13±3.21	38.12±2.33	37.23±3.7	37.98±3.6
SHMG (n=22)	47.05±3.15	43.16±2.79	40.18±3.28	38.2±4.1	38.56±3.3
P[1]	0.0000	0.0000	0.0000	0.6500	0.0692
Q1	1.0009	3.2215[a]	2.7517	0.1710	0.0548
Q2	3.3167	5.4437[b]	4.8958[b]	0.2497	2.3662
Q3	7.0441[b]	8.1513[b]	7.1776[b]	1.6607	3.1182
Q4	2.1398	1.9007	1.8579	0.0635	2.1995
Q5	5.8599[b]	4.8869[b]	4.3812[b]	1.4412	2.9505
Q6	4.1666[b]	3.3641[a]	2.8694[a]	1.4654	1.0294

[1]One-factor analysis of variance followed by SNK test. Q1: Q values between EG group and LMMG group; Q2: Q values between EG group and HMG group; Q3: Q values between EG group and SHMG group; Q4: Q values between LMMG group and HMG group; Q5: Q values between LMMG group and SHMG group; Q6: Q values between HMG group and SHMG group. [a]P<0.05; [b]P<0.01.

Differences of CST among four groups were statistically significient (P<0.001). There was negative relationship between CST and P1 amplitude, P1 amplitude density (r=-0.402, P<0.001; r=-0.261, P=0.003). There was positive relationship between CST and P1 implicit time (r=0.34, P<0.001) (Table 5, Figure 3).

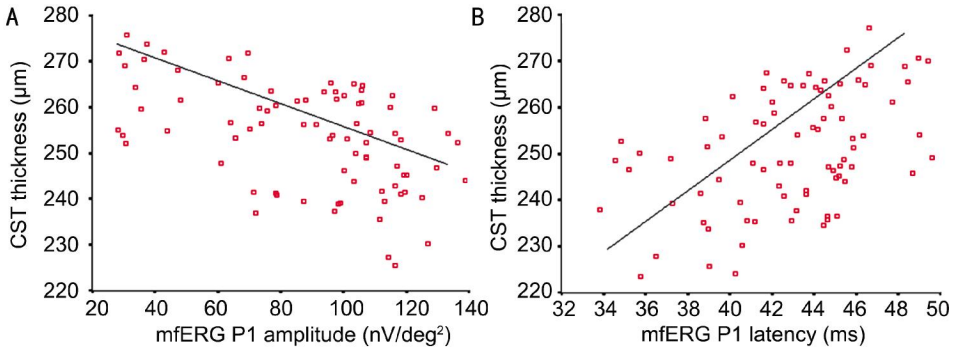

Figure 3 The relationship between CST and mfERG P1 parameters A: Relationship between CST and P1 amplitude; B: Relationship between CST and P1 implicit time.

Table 5 Correlation of the CST with the ring 1 mfERG parameters in myopia

Parameters	Pearson correlation coefficient	*P*
P1 amplitude density	-0.261	0.003
P1 amplitude	-0.402	＜0.001
P1 implicit time	0.34	＜0.001

DISCUSSION

ERG is an objective electrophysiological techniques and can be used to detect the changes of retinal function. ERG includes three types, flash ERG, pattern ERG and mfERG. Flash ERG reflects the function of entire retina, it is difficult to determine the lesion from the reaction waveform, and is not sensitive to small lesions. Pattern ERG response can be recorded locally, and can reflect macular function, but it need a long recording time, and the reaction amplitude is small. The mfERG can detect retinal visual function of 30° region, and locate the abnormal area of retinal function objectively with a relatively short time. In a first-order reaction, the results of mfERG reflect the function of retinal photoreceptor cells (mainly cones) and can be used for quantitative detection of macular function[9-10].

Using mfERG to detect the function of retina should consider the effction of age [11]. Anzai *et al* [12] founded the differences of N1 amplitude and P1 amplitude among different age groups were statistically significant. They also founded the differences of N1 implicit time and P1 implicit time among different age groups were statistically significant. The mfERG resoponse densities of older subjects were significantly lower than the young subjects, especially at the center of macular[11]. By comparision the differences of amplitude values of N1, P1 and N2 between <50y group and ≥50y group, Wu *et al* [13] founded the amplitude values of ≥50y group were significantly less than that of <50y age group. Possible reasons were with the increasing of age, the response of cells become slow. Age is not considered in the previous studies about the impact of myopia on mfERG. In this study, in order to avoid the impact of age on the findings, we select subjects with age between 18-35y. So our results primarily reflect the impact of myopia on mfERG.

With the increasing of myopia, P1 amplitude of each ring decreased. The differences of P1 amplitude among 4 groups were statistically significant in ring 1-5. With the increasing of myopia, P1 implicit time gradually extended. The differences of P1 implicit time among 4 groups were statistically significant in ring 1-3. But the differences of P1 implicit time among 4 groups were not statistically significant in ring 4 and ring 5. So we can conclude that amplitude was more sensitive than implicit time.

Studies about the relationship between mfERG and spectral domain OCT of non-pathological myopia were rare. In this study, we analyzed the relationship of CST and mfERG parameters. Our results showed there was negative relationship between CST and P1 amplitude, P1 amplitude density. There was positive relationship between CST and P1 implicit time. Our results showed that the changes in the central macular was correlated with the changes of retina function. First-order reaction of mfERG mainly detected the function of outer retina, especially the function of cone cell. The reason of the increasing of CST is the extension of the photoreceptor outer segments [14]. Li *et al* [15] repoted a significant decrease in foveal cone density with increasing axial length. Ischemia of the outer layers of the retina and retinal circulation disturbances due to eyeball elongation resulting in lower photoreceptor density in the fovea[16]. Azad *et al* [17] founded no statistically significant correlation was noted between CST and mfERG parameters. The reason is that myopic subjects were not included (refraction between ± 0.5 D). The corresponding relationship between each ring of mfERG and the location of retina was inconclusive currently, so studies on the relationship between function and structure of the peripheral retina is limited. With the development of equipment and related software, future work is expected to achieve the consistent studies of the changes in retinal function and structure.

Several hypotheses have been put forward to explain why altered ERG responses occur in physiologically myopic eyes. Pallin [18] suggested that ERG amplitudes reduced in subjects with myopia due to an increased ocular resistance from the electrical sources (the retina) and the electrodes. This

postulation is supported by findings of reduced ERG amplitudes in eyes which have resistive materials (*i.e.* increased ocular resistance) such as silicone oil injected into the vitreous cavity following surgery[19]. However, the ocular resistance theory was disputed by Chen *et al* [20] who suggested that the reduced ERG amplitude is likely to suggest a low retinal cell responsivity. It has also been suggested that other factors such as an increase in subretinal space or a change in the morphological profiles of the retinal cells due to an increase in axial length contribute to the decrease in ERG potentials in myopic eyes [21]. The reported lower amplitudes and longer latencies of the mfERG responses have also been interpreted as evidence of cone function loss, despite the lack of apparent myopic degeneration [20]. Other possible retinal processes that could explain the altered responses in myopia are in the dopaminergic system [22-23]. Dopamine levels are reduced in form-deprivation myopia [24]. Dopamine agonists have been shown to inhibit myopia[21,25]. Dopamine also can modifiy the spatial and dynamic properties of the ganglion cell responses, and alters contrast sensitivity[26].

The function of retinal photoreceptor cells of high myopes with normal vision and no obvious pathological changes has decreased significantly. Therefore, the application mfERG combined with other imaging techniques for patients with high myopia can find retinal changes earlier. This can predict the disease progression and provide an objective basis for the prevention of blindness. Future studies should include applications of different mfERG protocols that extract more subtle changes in retinal processing.

ACKNOWLEDGEMENTS

Conflicts of Interest: Song AP, None; **Yu T,** None; **Wang JR,** None; **Liu W,** None; **Sun Y,** None; **Ma SX,** None.

REFERENCES

1 He M, Zheng Y, Xiang F. Prevalence of myopia in urban and rural children in mainland China. *Optom Vis Sci* 2009;86(1):40-44.

2 Low W, Dirani M, Gazzard G, Chan YH, Zhou HJ, Selvaraj P, Au Eong KG, Young TL, Mitchell P, Wong TY, Saw SM. Family history, near work, outdoor activity, and myopia in Singapore Chinese preschool children. *Br J Ophthalmol* 2010;94(8):1012-1016.

3 Pan CW, Zheng YF, Anuar AR, Chew M, Gazzard G, Aung T, Cheng CY, Wong TY, Saw SM. Prevalence of refractive errors in a multiethnic Asian population: the Singapore epidemiology of eye disease study. *Invest Ophthalmol Vis Sci* 2013;54(4):2590-2598.

4 Atchison DA, Jones CE, Schmid KL, Pritchard N, Pope JM, Strugnell WE, Riley RA. Eye shape in emmetropia and myopia. *Invest Ophthalmol Vis Sci* 2004;45(10):3380-3386.

5 Cheng SC, Lam CS, Yap MK. Retinal thickness in myopic and non-myopic eyes. *Ophthalmic physiol Opt* 2010;30(6):776-784.

6 Abbott CJ, Grunert U, Pianta MJ, McBrien NA. Retinal thinning in tree shrews with induced high myopia: optical coherence tomography and histological assesment. *Vision Res* 2011;51(3):376-385.

7 Wolsley CJ, Saunders KJ, Silvestri G, Auderson RS. Investigation of changes in the myopic retina using multifocal electroretinograms, optical coherence tomography and peripheral resolution acuity. *Vision Res* 2008; 48(14): 1554-1561.

8 Fortune B, Johnson CA. Decline of photopic multifocal electroretinogram responses with age is due primarily to preretinal optical factors. *J Opt Soc Am A Opt Image Sci Vis* 2002;19(1):173-184.

9 Sun XY, Li JJ, Wang Y, Xu L. The effects of myopia on first-order kernels responses of multifocal electroretinogram. *Chin J Ocul Fundus Dis* 2006;22(2):103-105.

10 Luu CD, Lau AM, Lee SY. Multifocal electroretinogram in adults and children with myopia. *Arch Ophthalmol* 2006;124(3):328-334.

11 Langrova H, Zrenner E, Kurtenbach A, Seeliger MW. Age-related changes in retinal function tomography. *Invest Ophthalmol Vis Sci* 2008; 49(11):5024-5032.

12 Anzai K, Mori K, Ota M, Murayama K, Yoneya S. Aging of macular function as seen in multifocal electroretinograms. *Nippon Ganka Gakkai Zasshi* 1998;102(1):49-53.

13 Wu D, Liang J, Ma J. The characteristics of multifocal electroretinogram in normal subjects in China. *Zhonghua Yan Ke Za Zhi* 2001;37(2):98-103.

14 Liang H, Crewther DP, Crewther SG, Barila AM. A role for photoreceptor outer segments in the induction of deprivation myopia. *Vision Res* 1995;35(9):1217-1225.

15 Li KY, Tiruveedhula P, Roorda A. Intersubject variability of foveal cone photoreceptor density in relation to eye length. *Invest Ophthalmol Vis Sci* 2010;51(12):6858-6867.

16 Park S, Kim SH, Park TK, Ohn YH. Evaluation of structual and functional changes in non-pathological myopic fundus using multifocal electroretinogram and optical coherence tomography. *Doc Ophthalmol* 2013;126(3):199-210.

17 Azad R, Ghatak U, Sharma YR, Chandra P. Multifocal electroretinogram in normal emmetropic subjects: correlation with optical coherence tomography. *Indian J Ophthalmol* 2012;60(1):49-52.

18 Pallin O. Influence of axial length of the eye on the size of the recorded b-potential in the clinical single-flash electroretinogram. *Acta Ophthalmologica* 1969; 47(Suppl.): 1-57.

19 Doslak MJ. A theoretical study of the effect of silicone oil on the electroretinogram. *Invest Ophthalmol Vis Sci* 1988,29(12):1881-1884.

20 Chen JF, Elsner AE, Burns SA, Hansen RM, Lou PL, Kwong KK, Fulton AB. The effect of eye shape on retinal responses. *Clinical Vision Science* 1992;7(6):521-530.

21 Rohrer B, Spira AW, Stell WK. Apomorphine blocks form-deprivation myopiain chickens by a dopamine D2-receptor mechanism acting in retina or pigmented epithelium. *Vis Neurosci* 1993;10(3):447-453.

22 Morgan IG. The biological basis of myopic refractive error. *Clin Exp Optom* 2003;86(5):276-288.

23 Wallman J, Winawer J. Homeostasis of eye growth and the question of myopia. *Neuron* 2004;43(4):447-468.

24 Stone RA, Lin T, Laties AM, Iuvone PM. Retinal dopamine and form-deprivation myopia. *Proc Natl Acad Sci U S A* 1989;86(2):704-706.

25 Schmid KL, Wildsoet CF. Inhibitory effects of apomorphine and atropine and their combination on myopia in chicks. *Optom Vis Sci* 2004;81 (2): 137-147.

26 Witkovsky P. Dopamine and retinal function. *Doc Ophthalmol* 2004; 108(1):17-40.